

Calorimetry for active systems

Pritha Dolai,^{1,*} Christian Maes,¹ and Karel Netočný²

¹*Instituut voor Theoretische Fysica, KU Leuven, Belgium*

²*Institute of Physics, Czech Academy of Sciences, Prague, Czech Republic*

(Dated: August 3, 2022)

(Thermal) active systems are in physical contact with (at least) two reservoirs: one which is often chemical or radiative and source of low entropy, and one which can be identified with a thermal bath or environment in which energy gets dissipated. Perturbing the temperature, the heat capacity measures the excess heat in addition to the steady ever-existing dissipation. Simulating AC-calorimetry, we numerically evaluate the heat capacity for run-and-tumble particles in double-well and periodic potentials. Low-temperature Schottky-like peaks show the role of activity and indicate shape transitions, while regimes of negative heat capacity appear at higher propulsion speeds.

I. INTRODUCTION

The influence of heat on chemical reactions was already breaking ground in the 18-th century [1]. Yet, till around a century ago, physics understanding remained incomplete where it involved the specific heat of gases. That played a crucial role in the emergence of quantum mechanics and its first applications to condensed matter physics. Since then, heat capacity is often depicted as a material constant, only subject to changes by modifying constraints such as volume or by varying temperature or other intensive parameters and always to follow the rules of equilibrium thermodynamics. It is however natural to imagine that nonequilibrium features may play a role as well, as equipartition is easily violated by driving or active forces [2]. We do not have in mind here long transients as for instance in glasses [3], but focus on the steady nonequilibrium condition. For example, a tissue may change its heat capacity when it is acted upon by molecular motors, or a transmission

*Electronic address: pritha.dolai@kuleuven.be

device when undergoing random potential changes while maintaining relatively large heat or electric currents. Similarly and not thoroughly explored so far, heat capacity will differ between live matter and its unorganized mixture of molecules [4, 5].

Quantitative explorations of heat due to biological functioning or as function of metabolic rates and changes therein are studied under the heading of bioenergetics [6]. References on measuring heat production in bacterial reservoirs include [7–9]. In general however, not much got systematized on the theory side of condensed matter and nonequilibrium statistical mechanics. The same holds true for active (meta)materials where thermal properties and functionalities may depend on nonequilibrium driving [10, 11] and it is again important to quantify the relation between heat and temperature.

The present paper takes this question of defining and computing heat capacities to the paradigmatic case of active systems [12–15]. Active particle models only shadow the complex mechanisms of life or of materials that cannot be sustained in thermodynamic equilibrium but, combining exact results and simulation, they are capable of highlighting important phenomena.

In the following we start by presenting the main ingredients for nonequilibrium calorimetry, including a discussion on how to numerically compute or to measure experimentally heat capacities for driven or active systems. That is followed by prototypical examples featuring flashing potentials and run-and-tumble particles. In all cases, except for an exact calculation in Appendix A, we obtain the heat capacity by simulation, following the scheme of AC-calorimetry [16–18]. We investigate the role of propulsion speed and of tumbling or flashing rates on particles that are either confined or which move on a periodic landscape. The main results are visualized in plots of the heat capacity. In the end, we also consider the heat-related (quasi-)entropy for these systems.

Since we use classical diffusions we certainly do not probe the quantum regime for translation degrees of freedom. For run-and-tumble particles there is however the two-valuedness of the noise pushing the particles and the presence of barriers between minima in the potential may as well introduce an effective discreteness at low temperatures. It is still interesting here to observe features as a Schottky-like anomaly and a regime of negative heat-capacity where an increased environment temperature enhances the excess dissipation.

For simplicity we consider here translational motion only, ignoring e.g. activity-induced vibration or rotation. The dynamical variable is a scalar, like the position on the real line

without considering inertial degrees of freedom, and the irreversible work done on the particle is by the active forces or by flashing the potential. Thermal properties of active particles have of course been widely discussed, including [7, 9, 19–25], but so far heat capacities, the traditional window on “active” degrees of freedom, have not been calculated, let alone explored there.

II. OUT-OF-EQUILIBRIUM CALORIMETRY

We refer to [16, 26, 27] for the initial theory and basic examples of nonequilibrium heat capacities $C(T)$ as function of bath temperature T . The idea is to estimate the quasistatic heat excess δQ^{ex} after a small temperature change δT , while holding constant a given set of system and environment parameters:

$$C(T) = \frac{\delta Q^{\text{ex}}}{\delta T} \quad (1)$$

To measure or to compute that $C(T)$ we apply AC-calorimetry where we vary the bath temperature at a given frequency $\omega \neq 0$, e.g. $T_t = T + \delta T \sin \omega t$. After the system relaxes (in a time which we assume is short compared with the ratio of excess heat to steady power dissipation), we measure the heat flux $q(t)$ to find

$$q(t) = q^{(T)} + \delta T [\sigma_1(\omega) \sin(\omega t) + \sigma_2(\omega) \cos(\omega t)] \quad (2)$$

defining $\sigma_{1,2}(\omega)$ as the in- and out-phase components of the temperature-sensitivity of the dissipation. We assume that the temperature-heat admittance decays fast enough in time. The only difference with equilibrium calorimetry is that now the DC-part $q^{(T)}$ no longer vanishes. Around a steady nonequilibrium condition, the latter provides the dominant (for $\omega \rightarrow 0$) contribution to the heat flux, whereas the heat capacity (1) becomes the next correction. Indeed, the low-frequency asymptotics of the heat current (2) is

$$q(t) = q^T + \delta T [B(T) \sin(\omega t) - C(T) \omega \cos(\omega t)] \quad (3)$$

where $B(T)\delta T = q^{T+\delta T} - q^T$. That method, explained in [16, 28] but in essence going back to the work of Sullivan & Seidel in [17] and to [18] for equilibrium processes, is applied in each of the nonequilibrium model systems we consider below. See Appendix A for a brief introduction to nonequilibrium calorimetry relating it to steady-state thermodynamics.

Note that the heat current $q(t)$ may depend on various kinetic details and on control parameters. Indeed, stationary nonequilibrium systems are open, not only to the thermal bath but to all kinds of driving or influences from the outside or from hidden degrees of freedom. Yet, the essential changes in the heat current are caused by the occupation of the energy levels no longer following an equilibrium statistics. We emphasize here that the nonequilibrium contribution cannot be reduced to a simple “thermodynamic” form as it depends on kinetic aspects. E.g., even in the quasistatic regime, the excess heat over temperature does not need and typically will not be an exact differential [29, 30], except close-to-equilibrium [31–33].

III. ACTIVE GAS

Consider the one-dimensional overdamped diffusive dynamics with equation of motion

$$\gamma \dot{x}_t = v \sigma_t - U'(\eta_t, x_t) + \sqrt{2\gamma T} \xi_t \quad (4)$$

for the position x_t of effectively independent run-and-tumble particles (RTPs) with propulsion speed v in a flashing potential $U(\eta_t, x)$ under standard white noise ξ_t . The flashing is governed by a process or protocol η_t . The prime in U' denotes a derivative with respect to x . If moving on the circle we must have that U is periodic in x . The ambient temperature is T . We are assuming here that γ and v are not depending on the temperature, which is a serious simplification. Another modeling feature is that we consider, besides the thermal noise, only dichotomous noise σ_t , not depending on temperature or location of the particle: the $\sigma_t \in \{+1, -1\}$ is flipping at fixed rate $\alpha > 0$. To set the time-scale we put friction $\gamma = 1$.

The mean energy of the particle at time t is

$$E(t) = \langle U(\eta_t, x_t) \rangle \quad (5)$$

where the (process-)average at time t samples the noises in (4). Locomotion changes the position to $x + dx$, by which the energy changes as $U(\eta, x) \rightarrow U(\eta, x + dx)$. That energy change can be decomposed into heat and work done on the particle, as says the First Law of Thermodynamics. The instantaneous expected heat flux has therefore two sources: the direct change dU of the energy minus the work done on the particle. For dU we apply Itô’s Lemma at fixed η , $dU = (v\sigma - U'(\eta, x))U'(\eta, x) + TU''(\eta, x)$. On the other hand,

the expected work done on the particle for locomotion is $w(x; \sigma, \eta) = \sigma v(-U'(\eta, x) + \sigma v)$. Therefore, the heat flux from the thermal bath to the particle is the difference,

$$\begin{aligned} q(x; \sigma, \eta) &= dU - w(x; \sigma, \eta) \\ &= 2v\sigma U'(\eta, x) - (U'(\eta, x))^2 + TU''(\eta, x) - v^2 \end{aligned} \quad (6)$$

To compute the heat capacity through the steady heat flux (3), we thus need to evaluate

$$q(t) = \langle 2v\sigma_t U'(\eta_t, x_t) - U'^2(\eta_t, x_t) + T_t U''(\eta_t, x_t) - v^2 \rangle_t$$

for sufficiently large $t > 0$, where also the process average $\langle \cdot \rangle_t$ uses the slowly varying temperature $T_t = T + \delta T \sin \omega t$ to replace T in the strength of the thermal noise in (4).

A. Flashing potential

To start with an exactly solvable case we take propulsion speed $v = 0$ and $U(\eta, x) = k(1 + \varepsilon\eta)x^2/2$, $0 \leq \varepsilon \leq 1$, where $\eta = \pm 1$ is flipping randomly at rate α . We refer to Appendix A for the calculation. The stationary energy at fixed temperature T is $E^{(s)} = T/2$. It depends only on temperature, giving the (false) impression that the system partitions energy in the same way as in equilibrium. Yet the heat capacity becomes non trivial, though still temperature independent, and it reveals a fundamentally different thermal response than for a passive particle (see Fig. 4(a)):

$$C(T) = \frac{1}{2} \left[1 + \frac{\varepsilon^2(1 + 2z)}{(1 + z(1 - \varepsilon^2))^2} \right] \quad (7)$$

where the (dimensionless) persistence factor $z = k/(\alpha\gamma)$ appears. In Fig. 4(b) in Appendix A, we add the simulation result for a flashing double-well potential where $C(T)$ does depend on temperature.

B. Run-and-tumble in a periodic potential

Consider a RTP with position x_t on the circle of length L , and moving in a sinusoidal potential. The dynamics is given by (4) where $U(\eta, x) = E_0 \sin(2\pi x/L)$ is not flashing. We fix $L = 20$ in the simulations. We plot the frequency-dependent response (2) in Fig. 5(a) in Appendix B, for temperature $T = 0.3E_0$. In the small-frequency ($\omega \downarrow 0$) limit the out-of-phase amplitude $\sigma_2(\omega)$ is linear in ω and the proportionality constant is the heat capacity.

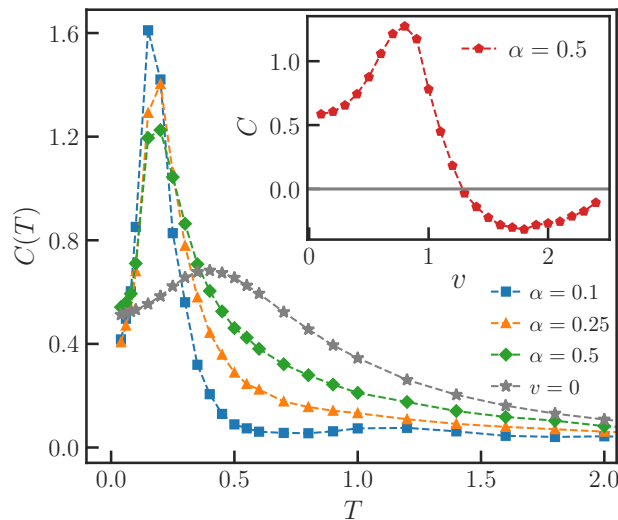


FIG. 1: Heat capacity of RTPs for different tumbling rates, moving in a sinusoidal potential with amplitude $E_0 = 1.0$ and propulsion speed $v = 1.0$. The grey line corresponds to the $v = 0$ (equilibrium) case. The inset shows the variation of the heat capacity with v for fixed $E_0 = 0.5$, tumbling rate $\alpha = 0.5$ and at temperature $T = 0.1$.

Fig. 1 shows that heat capacity for different tumbling rates. Interestingly, $C(T)$ has a peak at around $T \simeq E_0/5$. The peak decreases and shifts towards higher temperature for increased tumbling rate α . The peak value grows with the persistence to yield a significant magnification of the low-temperature heat capacity ($T < 0.3E_0$) with respect to equilibrium (= grey line in Fig. 1). For $\alpha \downarrow 0$, we find the heat capacity similar to what is e.g. shown in Fig. 1 in [26], and to the findings in [34] for active random walks on a ring. The appearance of a Schottky-like anomaly [35] for small enough v indeed shows the presence of a single energy scale E_0 in the potential. Of equal interest, from Fig. 1 inset, the heat capacity gets negative when the propulsion speed v is large enough to reach kinetic energies above the barrier height E_0 .

C. Run-and-tumble in a double-well potential

Run-and-tumble particles in one-dimension and subject to an external confining potential have been much studied for their static and dynamical properties; see e.g. [36, 37] and [38] for the non-Boltzmann stationary distribution at zero temperature. Heat capacities have

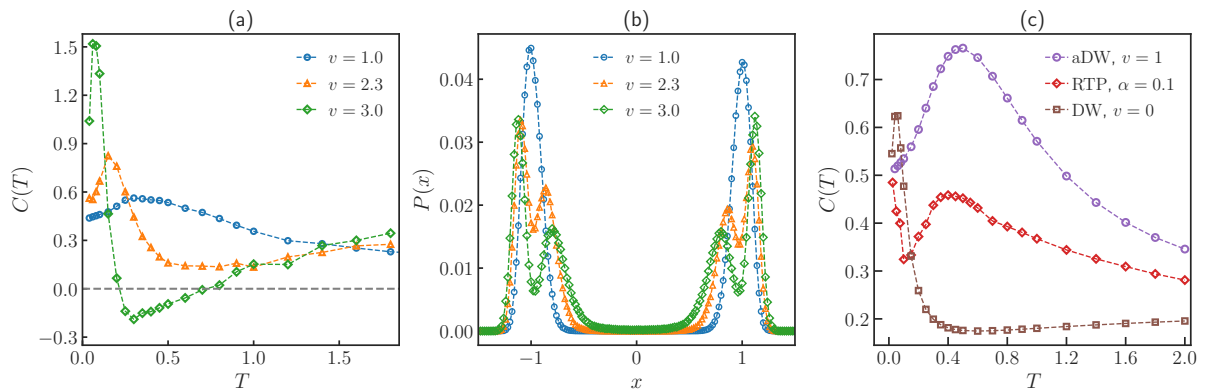


FIG. 2: (a) Heat capacity for RTPs in a double-well potential with barrier height $\Delta = 2.5$ for different propulsion speeds v at tumbling rate $\alpha = 0.5$. (b) Corresponding steady state occupation density $P(x)$ for different propulsion speeds. Here $E_0 = 10.0$, and $T = 0.1$. (c) Heat capacities for an asymmetric double well (upper curve), for RTPs in a double-well potential at $v = 1.0$, barrier height $\Delta = 0.25$ and $\alpha = 0.1$, and for a symmetric double well (lower curve). See around (8).

never been computed however.

Here we consider RTPs moving on a line and confined by the symmetric double-well potential $U(\eta, x) = U(x) = E_0(x^4/4 - x^2/2)$ in (4) (not flashing). The barrier height between the two wells is $\Delta = E_0/4$. As in equilibrium, that potential may arise as effective interaction in a mean-field description.

Fig. 2(a) gives the heat capacity for different propulsion speeds v . Again we see the appearance of negative heat capacities when v gets large compared to the barrier height Δ . Interestingly, we can also detect the zero-temperature shape transition, [36, 37, 39], from the behavior of the heat capacity at low temperature: Fig. 2(b) shows the stationary distribution and how it changes at $T = 0.1$ for the same parameters as in Fig. 2(a). When v is still small, the occupation is bimodal at low temperatures (corresponding to the two wells, as in equilibrium). As we increase v (going active), there appears a bimodality in each well, leading to four local maxima in the occupation distribution. That gets combined with a sharper and higher low-temperature peak in the heat capacity. And again negative heat capacities appear at large v as was the case in Fig. 1.

Finally, Fig. 2(c) shows a comparison between equilibrium and highly persistent RTPs. The upper curve is the heat capacity of an asymmetric (by v) double-well potential (aDW),

$$U(x) = E_0\left(\frac{x^4}{4} - \frac{x^2}{2}\right) + vx \quad (8)$$

and the lower curve has $v = 0$ (DW); see also [40]. For the two upper curves, the propulsion speed v is large so that $U(x, \pm)$ has a single minimum at $\pm x^*(v)$. For low temperatures and small tumbling rate α , the dynamics is quickly relaxing to the neighborhood of the potential minimum $\pm x^*$ and we find that the heat capacity of the RTPs resembles the DW-curve representing Gaussian fluctuations in an effective quadratic potential, $C \sim 1/2$. When temperature increases, the heat capacity qualitatively picks up the behavior of the aDW-curve as the passive fluctuations start to be governed by the subquadratic segment in (8). At high-T, we get fluctuations in an effective quartic potential, $C \sim 1/4$. Fig. 6 in Appendix B shows the heat capacity for a broader range of tumbling rates.

IV. ENTROPY

Entropy originates in the Clausius heat theorem, gets a statistical meaning as logarithmic measure of phase space volumes, and gives rise to statistical forces to govern variational principles. Such a protean entropy does not exist for genuine nonequilibria, [29, 30]. Yet, a heat-related entropy can be constructed, also for active systems, by defining the change ΔS in nonequilibrium *entropy*, without defining entropy as a state function:

$$\Delta S(T) = \int_{T_0}^T dT' \frac{C(T')}{T'} \quad (9)$$

for some reference (initial) temperature T_0 . We plot that change in Fig. 3 for RTPs in two different landscapes and for two tumbling rates. We only used the data for $C(T)$ (in Fig. 1 and Fig. 6) for temperatures $T > T_0 = 0.04$ and 0.025 respectively. As far as we know, those are the first plots of a nonequilibrium quasi-entropy for active systems.

We emphasize that (9) refers to a change in the temperature-direction. When changing the tumbling rate α at constant ambient temperature, there is a change in excess heat as well. We can understand it as a nonequilibrium latent heat $C(\alpha)$. As in (3), we obtain it by applying a sinusoidal modulation $\alpha(t) = \alpha + \sin(\omega t) \delta\alpha$ for which the heat current becomes

$$q(t) = q^\alpha - [a \sin(\omega t) - C(\alpha) \omega \cos(\omega t)] \delta\alpha + \mathcal{O}(\omega^2) \quad (10)$$

Fig. 5(b) in Appendix B depicts $C(\alpha)$ for $T = E_0/5$, showing a sharp increase for smaller tumbling rates α .

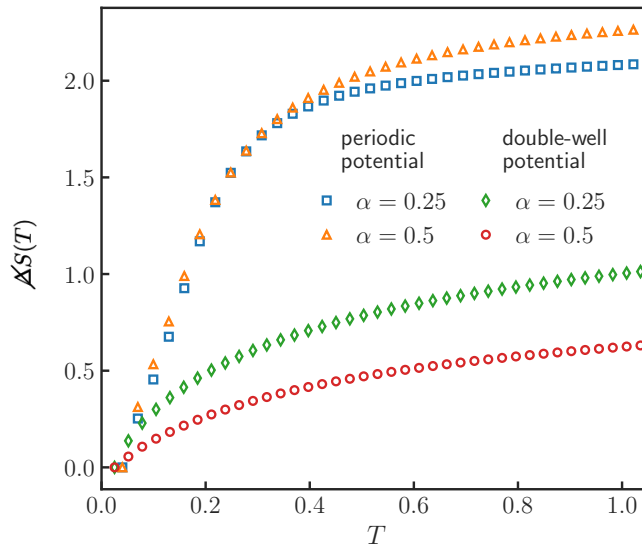


FIG. 3: Quasi-entropy (9) as function of temperature for RTPs moving in a sinusoidal potential (upper curves), and confined by a double-well potential (lower curves).

V. CONCLUSION

Far enough from equilibrium, entropy and its principles do not suffice at all to describe thermal susceptibility. Yet, the notion of heat capacity survives and describes how excess heat varies when changing environment temperature, and depends on activity parameters. Larger nonequilibrium amplitudes such as quantified by persistence time or flashing rate increase the heat capacity at low enough temperature; higher propulsion speeds may produce negative heat capacities in RTPs. Generally, the heat capacity reveals important aspects of the nonequilibrium dynamics in a way similar to measuring thermal properties for equilibrium systems to detect energy spectra. We also refer in that respect to [41] for an extended Nernst heat theorem.

Experiments using AC-calorimetry as numerically employed here, are very welcome to carry that program, to verify those predictions and hence to continue the old adage that *Even fire is ruled by numbers* [42] in the physics of active and living materials as well.

Appendix A: Flashing potential

We consider an overdamped diffusive particle in a one-dimensional flashing potential, following (4) with propulsion speed $v = 0$. An exactly solvable case is obtained for a

quadratic potential,

$$\gamma \dot{x}_t = -\partial_x U(\eta_t, x_t) + \sqrt{2\gamma T} \xi_t, \quad U(\eta, x) = \frac{k}{2}(1 + \varepsilon\eta)x^2 \quad (\text{A1})$$

where η_t is a standard dichotomous process ($\eta = \pm 1$) with persistence rate α . The parameter $\varepsilon \in [0, 1]$ prescribes the ratio by which the potential is turned off. For understanding the First Law, Eqs.(5)-(6), we take the x -component of the backward generator L , acting on function f as

$$L^{(x)}f = \gamma^{-1}(-U'\partial_x + T\partial_x^2)f = \gamma^{-1}[-k(1 + \varepsilon\eta)x\partial_x + T\partial_x^2]f \quad (\text{A2})$$

The full backward generator is $Lf(x, \eta) = L^{(x)}f(x, \eta) + \alpha[f(x, -\eta) - f(x, \eta)]$. Therefore,

$$\begin{aligned} \frac{d}{dt}\langle x^2 \rangle &= -2k\langle x^2 \rangle - 2k\varepsilon\langle \eta x^2 \rangle + 2T \\ \frac{d}{dt}\langle \eta x^2 \rangle &= -2k\varepsilon\langle x^2 \rangle - 2(k + \alpha\gamma)\langle \eta x^2 \rangle \end{aligned}$$

and under stationarity,

$$\langle x^2 \rangle^{(s)} = \frac{1 + z}{1 + z(1 - \varepsilon^2)} \frac{T}{k} \quad (\text{A3})$$

$$\langle \eta x^2 \rangle^{(s)} = -\frac{z\varepsilon}{1 + z(1 - \varepsilon^2)} \frac{T}{k} \quad (\text{A4})$$

where $z = k/(\alpha\gamma)$, a dimensionless persistence factor. Note that for flashing rate $\alpha \downarrow 0$, the variance (A3) is the sum of the variances corresponding to $\eta = \pm 1$, while the correlation (A4) remains different from zero for $\varepsilon \neq 0$. On the other hand, the stationary energy is

$$E^{(s)} = \frac{k}{2}(\langle x^2 \rangle^{(s)} + \langle \eta x^2 \rangle^{(s)}) = \frac{T}{2} \quad (\text{A5})$$

and depends only on temperature.

The (mean instantaneous) heat flux equals

$$q(x, \eta) = -L^{(x)}U = \gamma^{-1} \left[k^2(1 + \varepsilon^2)x^2 + 2\varepsilon k^2 \eta x^2 - kT(1 + \varepsilon\eta) \right] \quad (\text{A6})$$

Its stationary value

$$q^{(s)} = \langle q \rangle^{(s)} = \frac{kT}{\gamma} \frac{\varepsilon^2}{1 + z(1 - \varepsilon^2)} \quad (\text{A7})$$

is the steady heat flux. The quasipotential [26, 27] is

$$V(x, \eta) = \int_0^\infty dt \left[\langle q(X_t, \eta_t) | X_0 = x, \eta_t = \eta \rangle - q^{(s)} \right]$$

We can find it as the solution to the equation $(LV)(x, \eta) = q^{(s)} - q(x, \eta)$ (unique on the appropriate functional space, $\|Y\|^2 = \langle Y^2 \rangle^{(s)} < \infty$). Substituting the *Ansatz*

$$V = \tilde{V} - \langle \tilde{V} \rangle^{(s)}, \quad \tilde{V}(x, \eta) = cx^2 + d\eta x^2 + g\eta \quad (\text{A8})$$

we find the corresponding coefficients

$$c = \frac{k}{2} \frac{1 + \varepsilon^2 + z(1 - \varepsilon^2)}{1 + z(1 - \varepsilon^2)}, \quad d = \frac{k}{2} \frac{z\varepsilon(1 - \varepsilon^2)}{1 + z(1 - \varepsilon^2)}, \quad g = -\frac{T}{2} \frac{z\varepsilon}{1 + z(1 - \varepsilon^2)} \quad (\text{A9})$$

Furthermore,

$$\langle \tilde{V} \rangle^{(s)} = \frac{T}{2} \left[1 + \frac{\varepsilon^2(1 + 2z)}{(1 + z(1 - \varepsilon^2))^2} \right] \quad (\text{A10})$$

so that $U(\eta, x) - V(x, \eta)$ remains different from zero for $\alpha \downarrow 0$:

$$\lim_{\alpha \downarrow 0} V(x, \eta) = U(x, \eta) - \frac{T}{2} \left(1 + \frac{\varepsilon\eta}{1 - \varepsilon^2} \right)$$

Finally, the steady heat capacity is independent of temperature and equals

$$\begin{aligned} C &= -\left\langle \frac{\partial V}{\partial T} \right\rangle^{(s)} = \frac{\partial \langle \tilde{V} \rangle^{(s)}}{\partial T} - \left\langle \frac{\partial \tilde{V}}{\partial T} \right\rangle^{(s)} \\ &= \frac{1}{2} \left[1 + \frac{\varepsilon^2(1 + 2z)}{(1 + z(1 - \varepsilon^2))^2} \right] \end{aligned} \quad (\text{A11})$$

(Note that the last term on the first line is zero, since $\partial \tilde{V} / \partial T \propto \eta$ and $\langle \eta \rangle^{(s)} = 0$.)

We thus distinguish the following regimes:

- (1) $\underline{\varepsilon = 0}$: $q^{(s)} = 0$ and $C = \frac{1}{2}$ (equilibrium)
- (2) $\underline{\varepsilon = 1}$: $q^{(s)} = \frac{kT}{\gamma}$ and $C = 1 + z$ (“release-and-retract”)
- (3) $\underline{z \rightarrow 0}$: $q^{(s)} \rightarrow \frac{kT}{\gamma} \varepsilon^2$ and $C \rightarrow \frac{1}{2}(1 + \varepsilon^2)$ (vanishing persistence)
- (4) $\underline{\varepsilon < 1, z \rightarrow \infty}$: $q^{(s)} \rightarrow 0$ and $C \rightarrow \frac{1}{2}$ (infinite persistence $\alpha \downarrow 0$).

In Fig. 4(a) we plot the heat capacity as function of z for $\varepsilon = 1/2$. To contrast, Fig. 4(b) gives the heat capacity for a flashing symmetric double well,

$$U(\eta, x) = \frac{k}{2} \left(1 + \frac{\eta}{2} \right) \left(\frac{x^4}{4} - \frac{x^2}{2} \right), \quad \eta = \pm 1 \quad (\text{A12})$$

as in the left-hand equation of (A1). In contrast with the flashing harmonic potential, that double-well case cannot be solved exactly and the (nonequilibrium) heat capacity nontrivially depends on temperature.

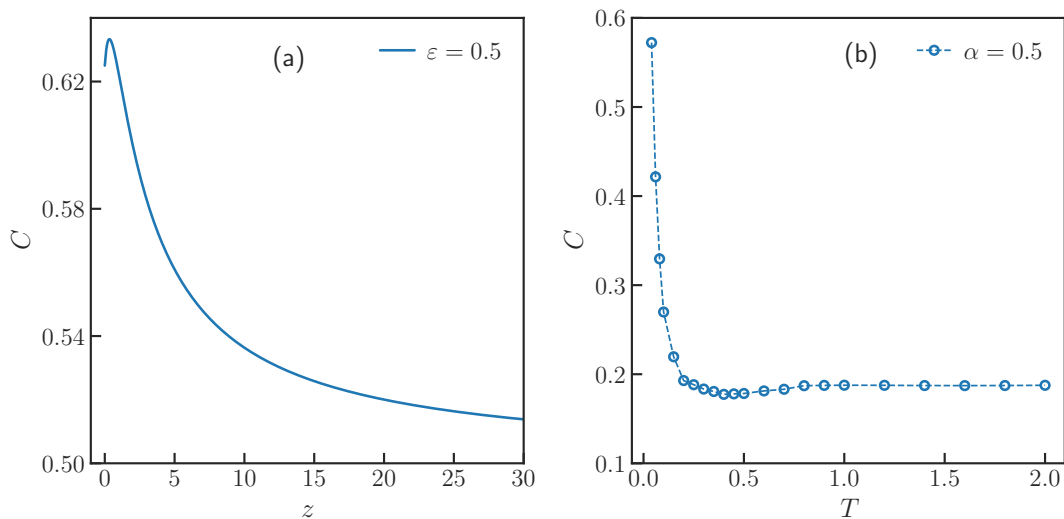


FIG. 4: (a) Heat capacity of a particle moving in a flashing harmonic potential, as in (A1), plotted as a function of persistence factor $z = k/(\alpha\gamma)$ for $\varepsilon = 0.5$. For $z \rightarrow 0$, $C \rightarrow 5/8$. (b) Heat capacity of a particle moving in the flashing symmetric double-well potential (A12), plotted as a function of temperature for flashing rate $\alpha = 0.5$.

Appendix B: Run-and-tumble particles

Run-and-tumble particles (RTPs) have a nonzero propulsion speed v in Eq. (4). There is no flashing of the potential U . The results there are obtained via AC-calorimetry, following the scheme of Eqs. (1)-(3); see also [16].

Fig. 5(a) shows the in- and out-of-phase components of the frequency-dependent heat current, defined in (2) for RTPs in a sinusoidal potential. The $\omega \downarrow 0$ of $\sigma_2(\omega)/\omega$ gives the heat capacity, as follows from AC-calorimetry.

Fig. 5(b) refers to (10), for the change of the excess heat per tumbling rate again for RTPs in the sinusoidal potential. The $C(\alpha)$ is a latent heat, as it refers to a constant temperature process.

Fig. 6 gives the heat capacity of RTPs in a double-well potential for different tumbling rates α . A broader peak shows at a temperature $T \simeq E_0/2$ for $\alpha \leq 0.5$. Compare with

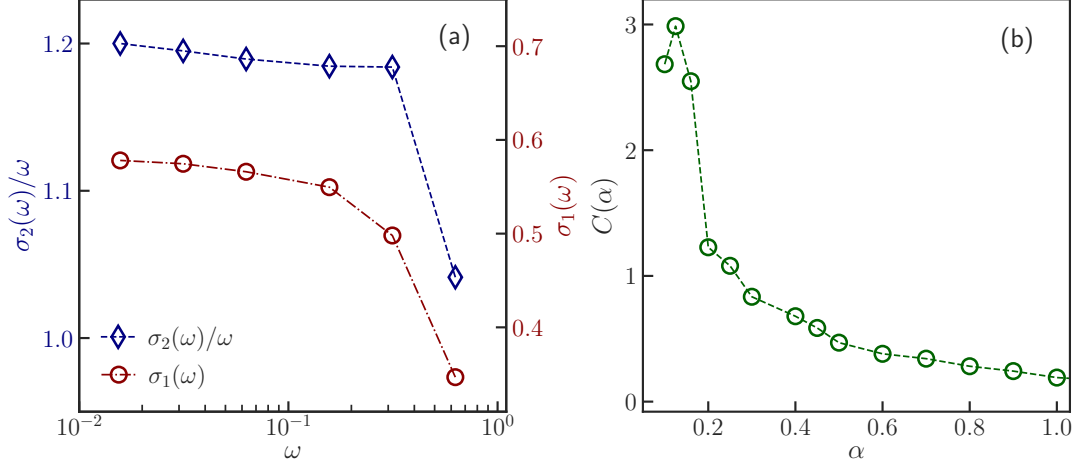


FIG. 5: RTPs in a sinusoidal potential. (a) cf. formulæ(2)–(3): the in-phase ($\sigma_1(\omega)$, as maroon circles) and out-of-phase ($\sigma_2(\omega)$, as blue diamonds) amplitudes of the heat current at $T = 0.15$, $\alpha = 0.5$. (b) cf. formula (10): change in excess heat per change in tumbling rate α at $T = 0.1$, $v = 1.0$ and $E_0 = 0.5$.

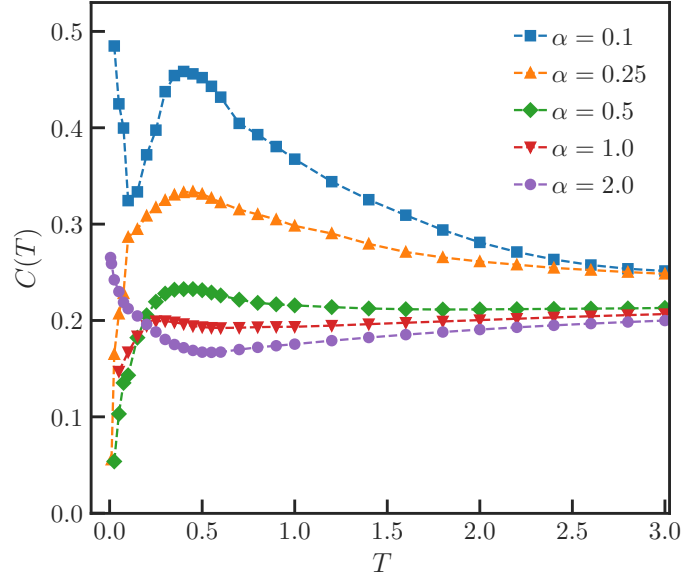


FIG. 6: Heat capacity of RTPs confined by a double-well potential plotted for different tumbling rates at $v = 1.0$ and barrier height $\Delta = 0.25$.

Fig. 2(c) for the small α -regime for large propulsion speed v .

-
- [1] Oeuvres de Lavoisier, Vol. II, p. 283.
 - [2] J.H. Jeans, The Distribution of Molecular Energy. Philosophical Transactions A **196**, 397–430 (1901).
 - [3] Xin-Yuan Gao, Hai-Yao Deng, Chun-Shing Lee, J. Q. You, Chi-Hang Lam, Emergence of two-level systems in glass formers: a kinetic Monte Carlo study. arXiv:2109.02275v5 [cond-mat.soft].
 - [4] *Handbook of Thermal Analysis and Calorimetry: From macromolecules to man*, Volume 4, Eds. Patrick Kent Gallagher, Michael E. Brown and Richard B. Kemp, Elsevier, 1999.
 - [5] *The nature of biological systems as revealed by thermal methods*, Volume 5 of Hot topics in thermal analysis and calorimetry, Ed. Dénes Lőrinczy, Springer, 2004.
 - [6] *Bioenergetics and Thermodynamics: Model Systems*, Nato Science Series C, volume 55, A. Braibanti (Ed.), Springer, 1980.
 - [7] H. P. Leiseifer, Heat production and growth kinetics of E. coli K12 from flow calorimetric measurements on chemostat cultures. Z Naturforsch C J Biosci. **4**, 1036–48 (1989).
 - [8] E. Rangel-Vargas, C.A. Gomez-Aldapa, R. Villagómez, E. M. Santos, J. Rodriguez-Miranda and J. Castro-Rosas, Growth measurement of Escherichia coli by differential scanning calorimetry. African Journal of Microbiology Research, 8(16), 1656–1662 (2014).
 - [9] Lee D. Hansen, R. S. Criddle and E. H. Battley, Biological calorimetry and the thermodynamics of the origination and evolution of life. Pure Appl. Chem. **81**, 1843 (2009).
 - [10] P. Fratzl, M. Friedman, K. Krauthausen and W. Schäffner, *Active Materials*, De Gruyter, 2021.
 - [11] J. O’Byrne, Y. Kafri, J. Tailleur and F. van Wijland, Time irreversibility in active matter, from micro to macro. Nat. Rev. Phys. **4**, 167 (2022).
 - [12] T. Maskow and S. Paufler, What does calorimetry and thermodynamics of living cells tell us? *Methods* **76**, 3 (2015).
 - [13] J. Tailleur and M. Cates, Statistical Mechanics of Interacting Run-and-Tumble Bacteria, Phys. Rev. Lett. **100**, 218103 (2008).
 - [14] M.C. Marchetti, J.F. Joanny, S. Ramaswamy, T. B. Liverpool, J. Prost, M. Rao, and R. A.

- Simha, Hydrodynamics of soft active matter. *Rev. Mod. Phys.* **85**, 1143 (2013).
- [15] C. Bechinger, R. Di Leonardo, H. Löwen, C. Reichhardt, G. Volpe, and G. Volpe, Active particles in complex and crowded environments. *Rev. Mod. Phys.* **88**, 045006 (2016).
- [16] C. Maes and K. Netočný, Nonequilibrium Calorimetry. *J. Stat. Mech.* 114004 (2019).
- [17] P.F. Sullivan and G. Seidel, Steady-State, ac-Temperature Calorimetry. *Phys. Rev.* **173**, 679 (1968).
- [18] J. K. Nielsen and J. C. Dyre, Fluctuation-dissipation theorem for frequency-dependent specific heat. *Phys. Rev. B* **54**, 15754 (1996).
- [19] F. Khodabandehlou, S.Krekels and I. Maes, Exact computation of heat capacities for active particles on a graph. arXiv:2207.11070v1 [cond- mat.stat-mech].
- [20] É Fodor, C. Nardini, M E. Cates, J. Tailleur, P. Visco, and F. van Wijland. How Far from Equilibrium is Active Matter? *Phys. Rev. Lett* **117**, 038103 (2016).
- [21] U. Marconi, A. Puglisi and C. Maggi, Heat, temperature and Clausius inequality in a model for active Brownian particles. *Sci Rep* **7**, 46496 (2017).
- [22] A. Puglisi and U.M. Bettolo Marconi, Clausius Relation for Active Particles: What Can We Learn from Fluctuations? *Entropy* **19**, 356 (2017).
- [23] P. Pietzonka and U. Seifert, Entropy production of active particles and for particles in active baths. *J. Phys. A: Math. Theor.* **51**, 01LT01 (2018).
- [24] G. Szamel, Stochastic thermodynamics for self-propelled particles. *Phys. Rev. E* **100**, 050603(R) (2019).
- [25] S. Krishnamurthy, S. Ghosh, D. Chatterji, R. Ganapathy and A. K. Sood, A micrometer-sized heat engine operating between bacterial reservoirs. *Nature Physics* **12**, 1134–1138 (2016).
- [26] E. Boksenbojm, C. Maes, K. Netočný, and J. Pešek, Heat capacity in nonequilibrium steady states. *Europhys. Lett.* **96**, 40001 (2011).
- [27] J. Pešek, E. Boksenbojm, and K. Netočný, Model study on steady heat capacity in driven stochastic systems. *Cent. Eur. J. Phys.* **10**, 692–701 (2012).
- [28] M. J. de Oliveira, Complex heat capacity and entropy production of temperature modulated systems. *J. Stat. Mech.* 073204 (2019).
- [29] D. Ruelle, Extending the definition of entropy to nonequilibrium steady states. *Proc. Natl. Acad. Sci.* **100**(6), 3054 (2003).
- [30] C. Maes, Nonequilibrium entropies. *Physica Scripta* **86**, 058509 (2012).

- [31] L. Bertini, D. Gabrielli, G. Jona-Lasinio and C. Landim, Thermodynamic transformations of nonequilibrium states. *J. Stat. Phys.* **149**, 773–802 (2012).
— Clausius inequality and optimality of quasistatic transformations for nonequilibrium stationary states. *Phys. Rev. Lett.* **110**, 020601 (2013).
- [32] C. Maes and K. Netočný, A nonequilibrium extension of the Clausius heat theorem. *J. Stat. Phys.* **154**, 188-203 (2014).
- [33] C. Maes and K. Netočný, Revisiting the Glansdorff–Prigogine Criterion for Stability Within Irreversible Thermodynamics. *J. Stat. Phys.* **159**, 1286–1299 (2015).
- [34] F. Khodabandehlou and I. Maes, Drazin-Inverse and heat capacity for driven random walks on the ring. arXiv:2204.04974v2 [math.PR].
- [35] E.S.R. Gopal, *Specific Heats at Low Temperatures*, The International Cryogenics Monograph Series, Springer New York, 1966.
- [36] U. Basu, S. N. Majumdar, A. Rosso, S. Sabhapandit and G. Schehr, Exact stationary state of a run-and-tumble particle with three internal states in a harmonic trap. *J. Phys. A: Math. Theor.* **53**, 09LT01 (2020).
- [37] A. Dhar, A. Kundu, S.N. Majumdar, S. Sabhapandit and G. Schehr, Run-and-tumble particle in one-dimensional confining potentials: Steady-state, relaxation and first-passage properties. *Phys. Rev. E* **99**, 032132 (2019).
- [38] K. Kitahara, W. Horsthemke, R. Lefever and Y. Inaba, Phase diagrams of noise induced transitions. *Prog. Theor. Phys.* **64**, 1233 (1980).
- [39] F.J. Sevilla, A.V. Arzola and E.P. Cital, Stationary superstatistics distributions of trapped run-and-tumble particles. *Phys. Rev. E* **99**, 012145 (2019).
- [40] H. Hasegawa, Specific heats of quantum double-well systems. *Phys. Rev. E* **86**, 061104 (2012).
- [41] F. Khodabandehlou, C. Maes and K. Netočný, A Nernst heat theorem for nonequilibrium jump processes. arXiv:2207.10313v1 [cond- mat.stat-mech].
- [42] *Et ignem regunt numeri*, citation attributed to Plato on the title page of *Théorie Analytique de la Chaleur* by Joseph Fourier, 1822.